



## Research article

# Prostate cancer small extracellular vesicles participate in androgen-independent transformation of prostate cancer by transferring let-7a-5p



Lin Lei <sup>a,c,1</sup>, Lijuan Yu <sup>a,b,d,\*</sup>, Weixiao Fan <sup>a,e</sup>, Xiaoke Hao <sup>a,e,\*\*</sup>

<sup>a</sup> Institute of Laboratory Medicine Center of Chinese People's Liberation Army (PLA), Xijing Hospital, Fourth Military Medical University (Air Force Medical University), China

<sup>b</sup> Department of Laboratory Medicine, Nanfang Hospital, Southern Medical University, China

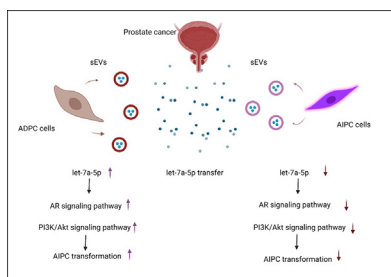
<sup>c</sup> Department of Clinical Laboratory Medicine, Xi'an Hospital of Traditional Chinese Medicine, China

<sup>d</sup> Krefting Research Centre, Institute of Medicine, University of Gothenburg, Sweden

<sup>e</sup> College of Medicine, Northwest University, China

## GRAPHICAL ABSTRACT

Prostate cancer sEVs participate in androgen-independent transformation of prostate cancer by transferring let-7a-5p.



## ARTICLE INFO

## Keywords:

Androgen-independent PCa

Androgen-dependent PCa

Castration-resistant PCa

Let-7a-5p

Androgen receptor signaling pathway

PI3K/Akt signaling pathway

## ABSTRACT

**Objectives:** Androgen deprivation therapy (ADT) is a standard treatment for advanced prostate cancer (PCa). However, after 2–3 years ADT treatment, prostate cancer inevitably transits from androgen-dependent PCa (ADPC) to androgen-independent PCa (AIPIC), which has a poor prognosis owing to its unclear mechanism and lack of effective therapeutic targets. Small extracellular vesicles (sEVs) play a vital role in the development of cancer. However, the role of PCa sEVs in the transformation of AIPIC remains poorly understood.

**Materials and methods:** Two different cell models were employed and compared. sEVs from ADPC cells (LNCaP) and AIPIC cells (LNCaP-AI + F cells) were isolated and characterized. After co-culture of LNCaP-AI + F sEVs with LNCaP cells and of LNCaP sEVs with LNCaP-AI + F cells, androgen-independent transformation was determined respectively. Mechanically, small RNA sequencing was performed. Androgen-independent transformation was examined by the upregulation and downregulation of miRNA and downstream pathways were analyzed.

**Results:** LNCaP-AI + F sEVs promoted the androgen-independent transformation of LNCaP cells. Interestingly, LNCaP sEVs exhibited a capacity to reverse the process. Let-7a-5p transfer was demonstrated. Furthermore, let-7a-

\* Corresponding author.

\*\* Corresponding author.

E-mail addresses: [lijuan.yu@gu.se](mailto:lijuan.yu@gu.se) (L. Yu), [haoxkg@fmmu.edu.cn](mailto:haoxkg@fmmu.edu.cn) (X. Hao).

<sup>1</sup> LL and LY contributed equally.

5p overexpression promotes the androgen-independent transformation and let-7a-5p down-regulation reverses the process. Androgen receptor (AR) and PI3K/Akt pathways were identified and demonstrated by both let-7a-5p regulation and PCa sEVs coculture.

**Conclusions:** PCa sEVs are intimately involved in the regulation of androgen-independent transformation of prostate cancer by transferring the key sEVs molecular let-7a-5p and then activating the AR and PI3K/Akt signaling pathways. Our results provide new perspectives for the development of sEVs and sEVs molecular targeted treatment approaches for AIPC patients.

## 1. Introduction

Prostate cancer (PCa) is the second leading cause of cancer death among male in 2020 [1]. Androgen deprivation therapy (ADT) has been the standard treatment method for PCa. However, after 2–3 years' ADT, most patients inevitably progress to the androgen-independent prostate cancer (AIPC) or castration-resistant PCa (CRPC), which derive from androgen-dependent prostate cancer (ADPC) and have poorer prognosis [2]. The molecular mechanisms controlling the transformation of ADPC to AIPC are still unclear.

Previous studies have shown that the progression of CRPC relies on androgen, which mainly exerts its biological effects via the androgen receptor (AR) [3, 4]. As the prostate differentiation factor, AR regulates the development of PCa via migrating into the nucleus and combining with AR-regulated genes such as prostatic specific antigen (PSA) [5]. The activation of the AR exists in the majority of CRPC patients and the expression of the AR protein was gradually reduced during the 120-day castration therapy period. However, AR expression level increased again in recurrent tumor [6], which indicates AR activation is closely related with AIPC or CRPC development. Moreover, another study also confirmed one of ADT mechanisms for therapy is that it inhibits androgen biosynthesis or AR activation [7]. Mechanisms for AR and other regulation pathways in CRPC are not fully understood.

Small extracellular vesicles (sEVs) are nanoscale extracellular vesicles containing miRNAs, mRNAs and proteins [8]. sEVs can initiate gene rearrangements and functional changes of target cells by transferring/shuttling miRNAs or mRNAs into target cells [9]. Previous studies have demonstrated that tumor sEVs play crucial roles in tumor development by shaping and modifying the tumor micro-environment [10, 11, 12, 13]. However, specific role of sEVs in AIPC transformation was poorly investigated.

In the present study we focused on the functional roles of sEVs in the progression of ADPC to AIPC and exploring potential signaling. Understanding the role played by sEVs in the progression of AIPC transformation could be crucial for development of additional therapies for CRPC.

## 2. Materials and methods

### 2.1. Cell lines and culture

ADPC cells LNCaP were obtained from American Type Culture Collection (ATCC, USA). AIPC cells LNCaP-AI + F (kind gift from professor Zhihua Tao, Zhejiang University, China) were induced by LNCaP cells in the androgen deprived environment with the androgen antagonist flutamide [14]. LNCaP cells were cultured in RPMI-1640 (Gibco, USA) supplemented with 15% fetal bovine serum (FBS). LNCaP-AI + F cell were cultured in phenol red free DMEM/F12 (Gibco, USA) supplemented with 15% charcoal stripped fetal bovine serum CS-FBS (BI, Israel) and 0.1 mol/L flutamide. All the media were supplemented with 100 U/mL penicillin and 100 µg/mL streptomycin (HyClone, USA). For further sEVs experiments, EVs-depleted FBS (BI, Israel) was used.

### 2.2. sEVs isolation and characterization

sEVs were collected from the cell culture supernatants by ultracentrifugation as previously described [13]. Briefly, supernatants were

harvested when the cells reached almost 80% confluence. Then the supernatant was centrifuged at 300 g for 10 min to eliminate cells, 2000 g for 10 min and 10,000 g for 30 min to remove cell debris and larger particles. Later, the supernatant was centrifuged twice at 100,000 g for 70 min and the pellets were dissolved in sterile PBS. BCA Protein assay kit (Pierce™, Thermo Fisher Scientific, USA) was applied for sEVs quantification, and sEVs morphology was analyzed using transmission electron microscopy (TEM) (JEM 1400plus, Japan). sEVs size distribution was analyzed by Zetasizer Nano ZS (Malvern, UK) and sEVs protein marker were detected by flow cytometer (BD, USA) and Western blotting.

### 2.3. Confocal microscopy analysis

When LNCaP cells confluent to 50–60%, LNCaP-AI + F sEVs labeled with the lipophilic phospholipid membrane dye Dil (Beyotime, China) were added and co-cultured for 48–72 h. After removal of the cell culture medium, the cells were gently washed with PBS three times, fixed with 4% paraformaldehyde for 20 min followed by an overnight incubation with E-cadherin primary antibody (Beyotime, China). The next day, cells were washed twice with PBS and incubated with Alexa Fluor 488-labeled secondary antibody (Beyotime, China) at room temperature for 2 h. Cells were washed again and then stained with DAPI for 5 min. The samples were observed on the FV10i laser confocal microscope (Olympus, Japan) with a 60x UIS2 SAPO air objective.

### 2.4. Western blotting analysis

sEVs (10 µg) or cell proteins (20–50 µg) were diluted in a loading buffer (Beyotime, China), heated at 100 °C for 5 min, centrifuged 12000 g for 10 min, loaded onto gels and electrophoresed (90 V for 25 min, then changed to 120 V 45 min). The iBlot (Invitrogen, USA) setting procedure was used to transfer membranes. Blocking buffer (Odyssey, USA) was used for 60 min before the incubation with primary antibodies at 4 °C overnight. TBS wash (3–5 min) performed before incubation of secondary antibodies at room temperature for 60 min in the dark; odyssey infrared scanning was performed. The following primary antibodies were used: Alix, AR, PSA, Akt, p-Akt (1:1000; Cell Signalling Technology, USA) and β-actin (1:1000; Sigma, USA).

### 2.5. Flow cytometry

sEVs were diluted in sterile PBS (100 µL) and incubated on ice with 20 µL fluorescent antibody conjugated aldehyde/sulfate latex beads (Invitrogen, USA) for 30 min. Unstained sEVs was used as negative control (NC). Labeling was performed against CD63 and CD81 and the experiment was performed in duplicates. The sorting was performed following the instrument operating procedures on FACS Canto II flow cytometer (BD, USA).

### 2.6. Sequencing and identification of sEVs miRNAs

sEVs miRNA sequencing was conducted by RiboBio Company (Guangzhou, China) using the HiSeq 2500 instrument (Illumina, USA). miRNeasy Serum/Plasma Kit (QIAGEN, Germany) was used to extract sEVs total RNA from isolated sEVs. The Mir-X™ miRNA First Strand Synthesis Kit (Takara, Japan) was used to complete the reverse

transcription reaction on the T100 Thermal Cycler (BIO-RAD, USA). SYBR<sup>®</sup> Premix Ex Taq<sup>™</sup> II (Takara) was used to PCR on the CFX96 Real-Time system (BIO-RAD). All sEVs miRNAs primers were obtained from RiboBio (cel-miR-39 was used as a control). Total cellular RNA was extracted using TRIzol (U6 RNA was used as a control).

### 2.7. Quantitative Real-time PCR (qRT-PCR)

cDNA was synthesized with a reverse-transcription kit (Takara, Japan). Quantitative analysis was performed using the SYBR<sup>®</sup> Premix Ex Taq<sup>™</sup> II (Takara, Japan) on CFX96 Real-Time system (BIO-RAD) according to the manufacturer's instructions. AR, PSA mRNA qPCR primers were synthesized by Sangon (Shanghai, China) and GAPDH was used as internal control.

### 2.8. Cell proliferation assay

The cells were seeded into the 96-well plates in the appropriate density. Cell density was checked at different time points (0, 24, 48, and 72 h) adding 10  $\mu$ L of CCK-8 reagent (Dojindo, Japan) to cell culture medium incubated at 37 °C for 1 h; then, the OD 450 nm was measured by a microplate reader.

### 2.9. Cell cycle analysis

After 48 h co-culture or transfection, cells were digested with 0.25% trypsin and centrifuged at 300 rpm/min for 5 min. Then, 1 mL of 75% ethanol was added to fix cells. After overnight incubation at 4 °C in 75% ethanol, cells were washed in PBS and resuspended in 0.5 mL propidium iodide (PI) for 30 min, then cell cycle was analyzed by Flow Cytometry (BD, USA).

### 2.10. Cell transfection

LNCAp cells were transfected with 50 nM, 100 nM mimic negative control miRNAs (mimic NC) and 50 nM, 100 nM let-7a-5p mimic. LNCAp-AI + F cells were transfected with 100 nM, 150 nM inhibitor negative control (inhibitor NC) and 100 nM, 150 nM let-7a-5p inhibitor. Cells were seeded into a 6-well plate at 30% confluence, and the transfection was performed when the cells reached 70–80% confluence with riboFECT CP Transfection Kit (Riobio, China).

### 2.11. Statistical analysis

All data are presented as means  $\pm$  SEM. Comparisons were performed using t-test or one-way ANOVA test implemented in GraphPad Prism 7.0.  $P < 0.05$  was considered statistically significant.

## 3. Results

### 3.1. Identification of PCa cell models and characterization of PCa derived sEVs

Firstly, we intended to investigate the difference between ADPC cells (LNCAp) and AIPC cells (LNCAp-AI + F) in androgen-deprived environment. We cultured the LNCAp cells and LNCAp-AI + F cells in androgen-deprived environment for 72 h. CCK-8 assay indicated a significantly increased proliferation of LNCAp-AI + F cells compared to LNCAp cells at 72 h ( $P < 0.001$ ; Figure 1A). Flow cytometry showed that in LNCAp-AI + F cells there was a higher rate in S-phase ( $P < 0.001$ ) and a lower rate in G0-G1 phase ( $P < 0.01$ ) (Figure 1B). Western blotting analysis showed the AR expression level was significantly up-regulated ( $P < 0.001$ ) in LNCAp-AI + F cells compared with LNCAp cells; whereas the expression of PSA protein level was obviously down-regulated ( $P < 0.001$ ) (Figure 1C).

To determine whether sEVs influence the castration resistance in PCa cells, we firstly isolated the sEVs from the culture supernatant by ultracentrifugation. We found a large amount of lipid bilayer membrane vesicles with size ranged 30–150 nm by transmission electron microscopy (TEM) (Figure 1D). Quantification of isolated vesicles size revealed that the mean diameter was in the range of 30–120 nm (Figure 1E). To further confirm the nature of the isolated vesicles, we analyzed sEVs marker by western blotting, sEVs protein Alix was detected (Figure 1F). Flow cytometry also revealed the presence of sEVs markers CD63 and CD81 (Figure 1G). Taken together, these results confirmed that the isolated vesicles were sEVs.

Furthermore, we tested the expressions of PCa cells sEVs specific proteins. Western blotting analysis showed the AR expression level was significantly up-regulated in LNCAp-AI + F sEVs compared with LNCAp sEVs; whereas the expression of PSA protein level was obviously down-regulated (Figure S1A). qRT-PCR showed higher AR mRNA expression ( $P < 0.001$ ) and lower PSA mRNA expression ( $P < 0.01$ ) in LNCAp-AI + F sEVs (Figure S1B).

### 3.2. sEVs derived from AIPC cells promote the castration resistance of ADPC cells

To reveal whether sEVs derived from AIPC cells had the ability to transfer castration resistance to ADPC cells, we co-cultured LNCAp cells with LNCAp-AI + F sEVs in androgen-deprived environment. First, we analyzed the expression of AR and PSA by Western blotting and qRT-PCR. As shown in Figure 2A, both the expression of AR and PSA protein significantly increased. qRT-PCR results showed that AR mRNA and PSA mRNA expression also significantly increased (Figure 2B). These results indicated that sEVs derived from AIPC cells can activate AR signaling pathway.

Subsequently, we investigated whether sEVs derived from AIPC cells could promote the proliferation of ADPC cells under androgen-deprived environment. The CCK-8 assay results indicated that 10  $\mu$ g/mL LNCAp-AI + F sEVs could increase cell growth, but due to the lower effective concentration, statistics analysis showed no significance, whereas 20  $\mu$ g/mL, 30  $\mu$ g/mL LNCAp-AI + F sEVs could obviously stimulate LNCAp cell proliferation (Figure 2C). And meanwhile, a dose dependent reaction was observed between 10  $\mu$ g/mL and 30  $\mu$ g/mL groups (Figure 2C). Flow cytometry of LNCAp cells treated with 20  $\mu$ g/mL LNCAp-AI + F sEVs revealed a higher rate of cells in S-phase ( $P < 0.001$ ) and a lower rate of cells in G0-G1 phase ( $P < 0.01$ ) (Figure 2D). These results indicated that sEVs derived from AIPC cells promote the development of castration resistance in ADPC cells.

### 3.3. sEVs derived from ADPC cells reverse the castration resistance of AIPC cells

Next, we investigated the roles of ADPC sEVs on AIPC cells. After co-culture LNCAp-AI + F cells with LNCAp sEVs in androgen-deprived environment, western blotting analysis showed that AR protein expression decreased at different time points within 24 h (Figure 3A). The results indicated that sEVs derived from ADPC cells can inhibit the activation of AR signaling pathway in the development of castration resistance of AIPC cells. Subsequently, using a CCK-8 assay we observed a decreased cell growth rate under androgen-deprived medium co-culturing LNCAp-AI + F cells with 10  $\mu$ g/mL, 20  $\mu$ g/mL, 30  $\mu$ g/mL sEVs derived from LNCAp cells up to 72 h, which displayed sEVs dose-dependent (Figure 3B). After 48 h co-culture, flow cytometry showed that LNCAp-AI + F cells treated with 20  $\mu$ g/mL sEVs derived from LNCAp cells exhibited a higher rate of cells in G0-G1 phase ( $P < 0.01$ ), a lower rate of cells in S phase ( $P < 0.001$ ) compared to control (PBS-treated) LNCAp-AI + F cells in castration condition (Figure 3C). These results suggested sEVs derived from ADPC cells can reverse the castration resistance of AIPC cells.

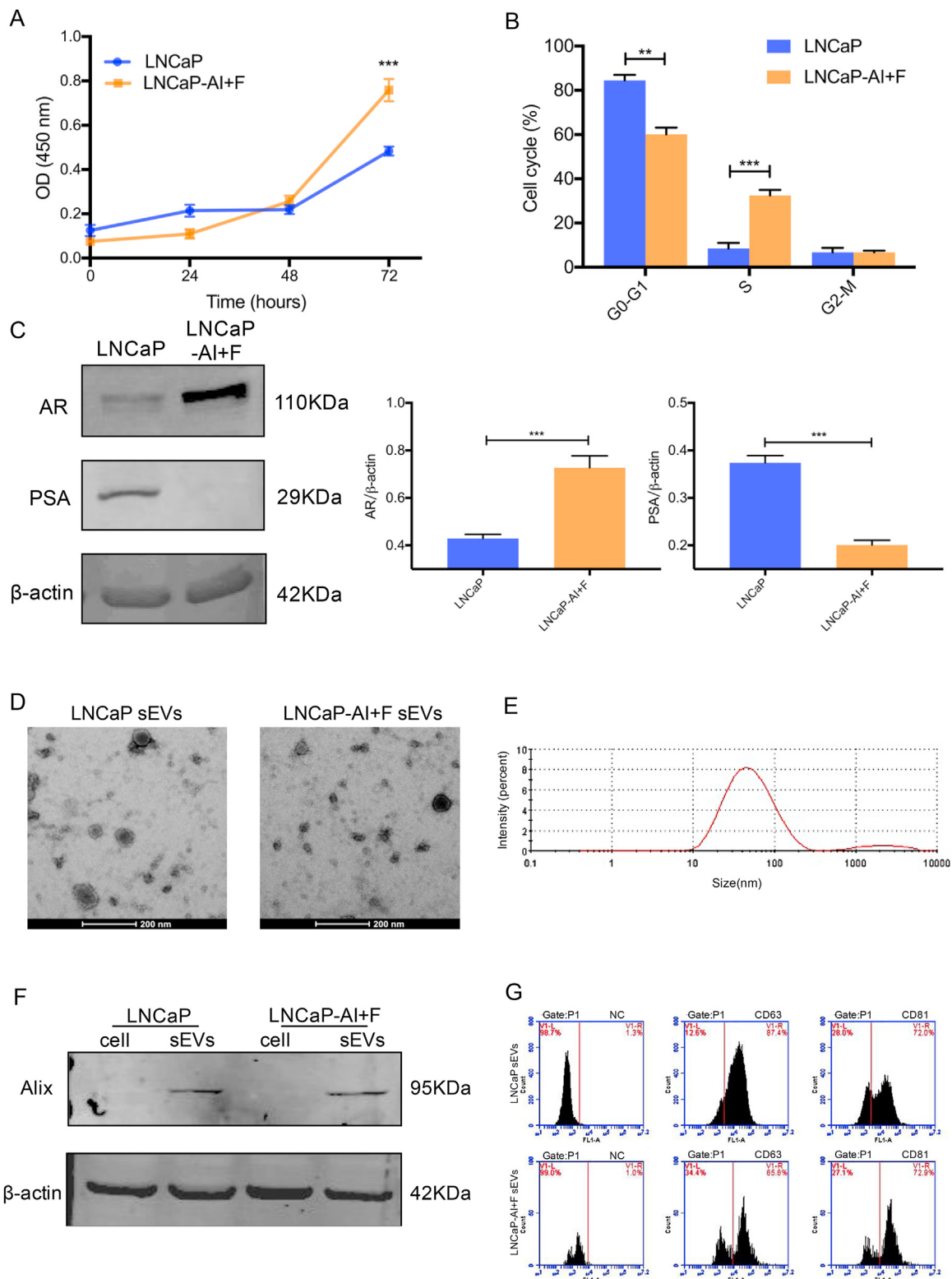


**Figure 1.** Characterization of LNCaP and LNCaP AI + F cells and sEVs. (A) CCK-8 assay of the proliferation of LNCaP cells and LNCaP-AI + F cells at 0, 24, 48, and 72 h in an androgen-deprived environment. (B) Flow cytometry analysis of the cell cycle distributions of LNCaP cells and LNCaP-AI + F cells at 72 h in an androgen-deprived environment. (C) Expression levels of AR and PSA proteins in LNCaP cells and LNCaP-AI + F cells determined by western blotting. Original gel data in Supplementary Materials (Figure S3). (D) Transmission electron microscopic images of sEVs isolated from LNCaP and LNCaP-AI + F cells. Scale bar:200 nm (E) Average size distribution of isolated sEVs. (F) Alix protein level was analysed by western blotting. (G) Flow cytometry analysis of the sEVs surface markers CD63 and CD81. Original gel data in Supplementary Materials (Figure S4). sEVs: small extracellular vesicles. Data were analyzed using *t*-test. \*,  $P < 0.05$ ; \*\*,  $P < 0.01$ ; \*\*\*,  $P < 0.001$ .

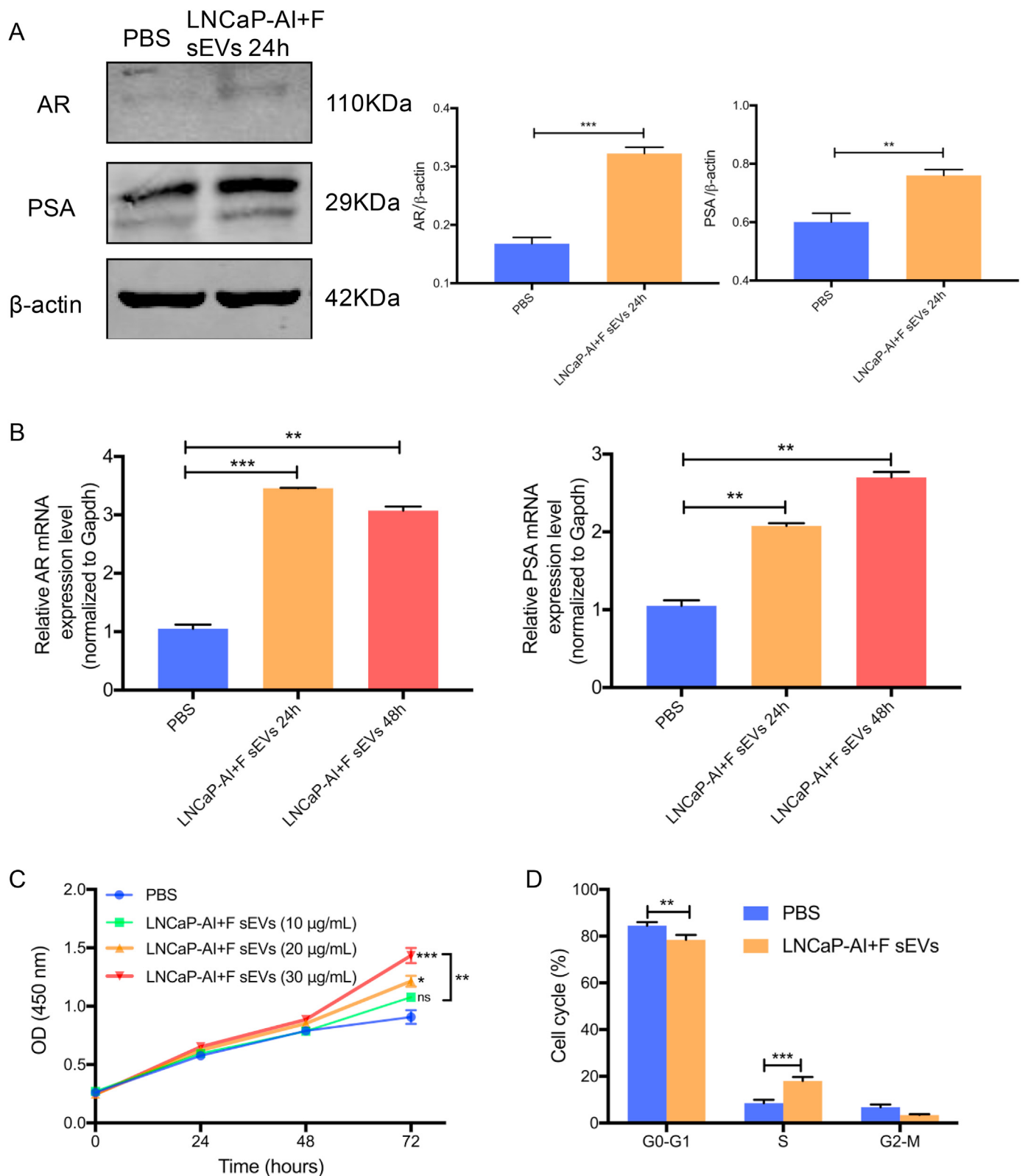


**Figure 2.** LNCaP-AI + F sEVs promote AIPC transformation. (A) Western blotting analysis and quantification of AR and PSA protein expressions in LNCaP cells co-cultured with LNCaP-AI + F sEVs for 24 h in an androgen-deprived environment. Original gel data in Supplementary Materials (Figure S5). (B) qRT-PCR analysis of the relative expression of AR and PSA mRNA in LNCaP cells co-cultured with LNCaP-AI + F sEVs for 24 or 48 h in an androgen-deprived environment. (C) CCK-8 assay of the proliferation of LNCaP cells co-cultured with 10 µg/mL, 20 µg/mL, 30 µg/mL LNCaP-AI + F sEVs for 0, 24, 48, and 72 h in an androgen-deprived environment. (D) Cell cycle distributions of LNCaP cells co-cultured with 20 µg/mL LNCaP-AI + F sEVs for 48 h were analysed by flow cytometry in an androgen-deprived environment. sEVs: small extracellular vesicles. Data were analyzed using *t*-test (A, D) and one-way ANOVA with multiple-comparisons test (B, C). \*,  $P < 0.05$ ; \*\*,  $P < 0.01$ ; \*\*\*,  $P < 0.001$ .

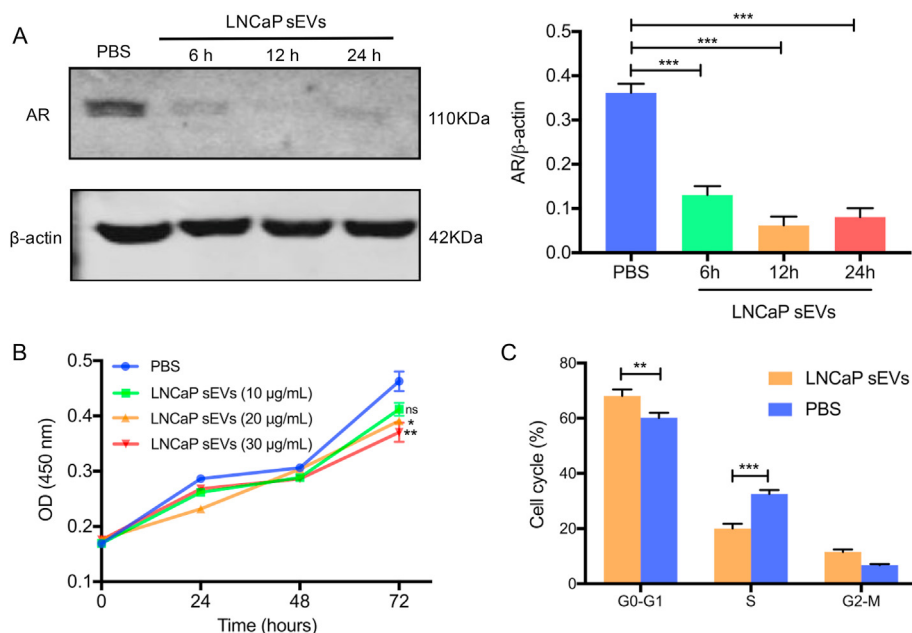


**Figure 3.** LNCaP sEVs can reverse AIPC transformation. (A) Western blotting analysis of AR expression in LNCaP-AI + F cells co-cultured with LNCaP sEVs for 6, 12, and 24 h in an androgen-deprived environment. Original gel data in Supplementary Materials (Figure S6). (B) CCK-8 assay of the proliferation of LNCaP-AI + F cells co-cultured with 10 µg/mL, 20 µg/mL, 30 µg/mL LNCaP sEVs for 0, 24, 48, and 72 h in an androgen-deprived environment. (C) The cell cycle distributions of LNCaP-AI + F cells co-cultured with 20 µg/mL LNCaP sEVs for 48 h analysed by flow cytometry in an androgen-deprived environment. sEVs: small extracellular vesicles. Data were analyzed using *t*-test (C) and one-way ANOVA with multiple-comparisons test (A, B). \*,  $P < 0.05$ ; \*\*,  $P < 0.01$ ; \*\*\*,  $P < 0.001$ .

### 3.4. Let-7a-5p was transferred between PCa cells

To explore the underlying mechanism on sEVs regulating the emergence of castration resistance of ADPC cells, we used high-throughput sequencing to analyze the differential expressed miRNAs profiling between LNCaP sEVs and LNCaP-AI + F sEVs. Taking  $|\log_2(\text{fold change})| \geq 1$  as the threshold for the identification of differentially expressed sEVs miRNAs (Figure 4A), we selected 147 sEVs miRNAs ( $P < 0.01$ ) and 67 sEVs miRNAs ( $0.01 \leq P < 0.05$ ). Finally, we screened out 18 differentially expressed sEVs miRNAs, among which 16 sEVs miRNAs showed higher expression and two showed significantly lower expression in LNCaP-AI + F sEVs (Figure 4B). qRT-PCR results showed that the relative expression of let-7a-5p was higher in LNCaP-AI + F sEVs (Figure 4C), as well as in LNCaP-AI + F cells (Figure 4D). Interestingly, we found an eight-fold up-regulation in LNCaP-AI + F sEVs and a four-fold up-regulation in LNCaP-AI + F cells, which indicated the possible let-7a-5p sorting to sEVs.

Next, we investigated whether sEVs mediated let-7a-5p transfer occurs in between cells. After co-culturing LNCaP cells with Dil-labelled LNCaP-AI + F sEVs for 48 h, the sEVs were taken up by recipient cells (Figure 4E). After LNCaP cells were treated with LNCaP-AI + F sEVs, we found that let-7a-5p expression was higher than that in PBS-treated LNCaP cells (Figure 4F). The let-7a-5p expression was lower in LNCaP-AI + F cells treated with LNCaP sEVs (Figure 4G). Taken together, these results indicate that sEVs can transfer let-7a-5p between PCa cells.

### 3.5. Let-7a-5p regulates AR signaling and castration resistance in PCa cells

let-7a-5p mimic and let-7a-5p inhibitor were employed to investigate the role of let-7a-5p in AIPC progression. qPCR results showed that let-7a-5p expression was upregulated in LNCaP cells transfected with the let-7a-5p mimic (Figure 5A), while let-7a-5p expression was downregulated in LNCaP-AI + F cells transfected with the let-7a-5p inhibitor (Figure 5B). Western blotting showed that the overexpression of let-7a-5p in LNCaP cells upregulated AR and PSA proteins expression (Figure 5C); in contrast, let-7a-5p downregulation in LNCaP-AI + F cells decreased AR protein expression (Figure 5D). These results indicated that let-7a-5p regulates the activation of the AR signaling pathway in the development of castration resistance in AIPC cells. Further, the overexpression of let-7a-5p could increase the proliferation of LNCaP cells and showed mimics dose-dependent, as determined by a CCK-8 assay

(Figure 5E) and could increase the rate of cells in the S phase and decrease rate of cells in the G0-G1 phase, as determined by flow cytometry (Figure 5F). However, let-7a-5p downregulation slow down the proliferation in LNCaP-AI + F cells and displayed similar inhibitor dose-dependent (Figure 5G), with a notably higher rate of cells in the G0-G1 phase and a lower rate of cells in the S phase (Figure 5H). These results implied that let-7a-5p regulates the development of castration resistance in PCa cells.

### 3.6. PCa sEVs encapsulating let-7a-5p regulate the PI3K/Akt signaling pathway

AR has been historically considered the most important target to control CRPC [15, 16]. Studies have further demonstrated that the AR signaling and the PI3K/AKT/mTOR pathway cross-regulates each other [4, 15, 16, 17]. So, our previous data pushed us to further detect the expression of PI3K/Akt signaling pathway. Western blotting results showed that let-7a-5p overexpression increased the ratio of *p*-Akt/Akt in LNCaP cells (Figure 6A), whereas let-7a-5p downregulation induced a relatively lower ratio of *p*-Akt/Akt in LNCaP-AI + F cells (Figure 6B). Western blotting results demonstrated that *p*-Akt protein expression and the *p*-Akt/Akt ratio increased in LNCaP cells treated with LNCaP-AI + F sEVs within 48 h (Figure 6C). Alternatively, *p*-Akt protein expression and the *p*-Akt/Akt ratio decreased in LNCaP-AI + F cells treated with LNCaP sEVs at 24 h (Figure 6D). Thus, as expected, PCa sEVs encapsulating let-7a-5p regulates the activation of the PI3K/Akt signaling pathway.

## 4. Discussion

The transformation from ADPC to AIPC, which has limited therapeutic treatments and is often aggressive, eventually induces PCa incurable and lethal [18]. Hence, we urgently need to clarify the underlying mechanisms on the transformation. Herein, we explored the regulation of PCa sEVs during the transformation from ADPC to AIPC. We found that sEVs derived from AIPC cells (LNCaP-AI + F) promote the AIPC transformation, and in contrast, surprisingly, sEVs derived from ADPC cells (LNCaP) can reverse the transformation. Furthermore, we found PCa sEVs delivering let-7a-5p regulated the AIPC transformation by activating AR signaling pathway and PI3K/Akt pathway, and subsequently regulated the proliferation of PCa cells. Our findings uncovered a

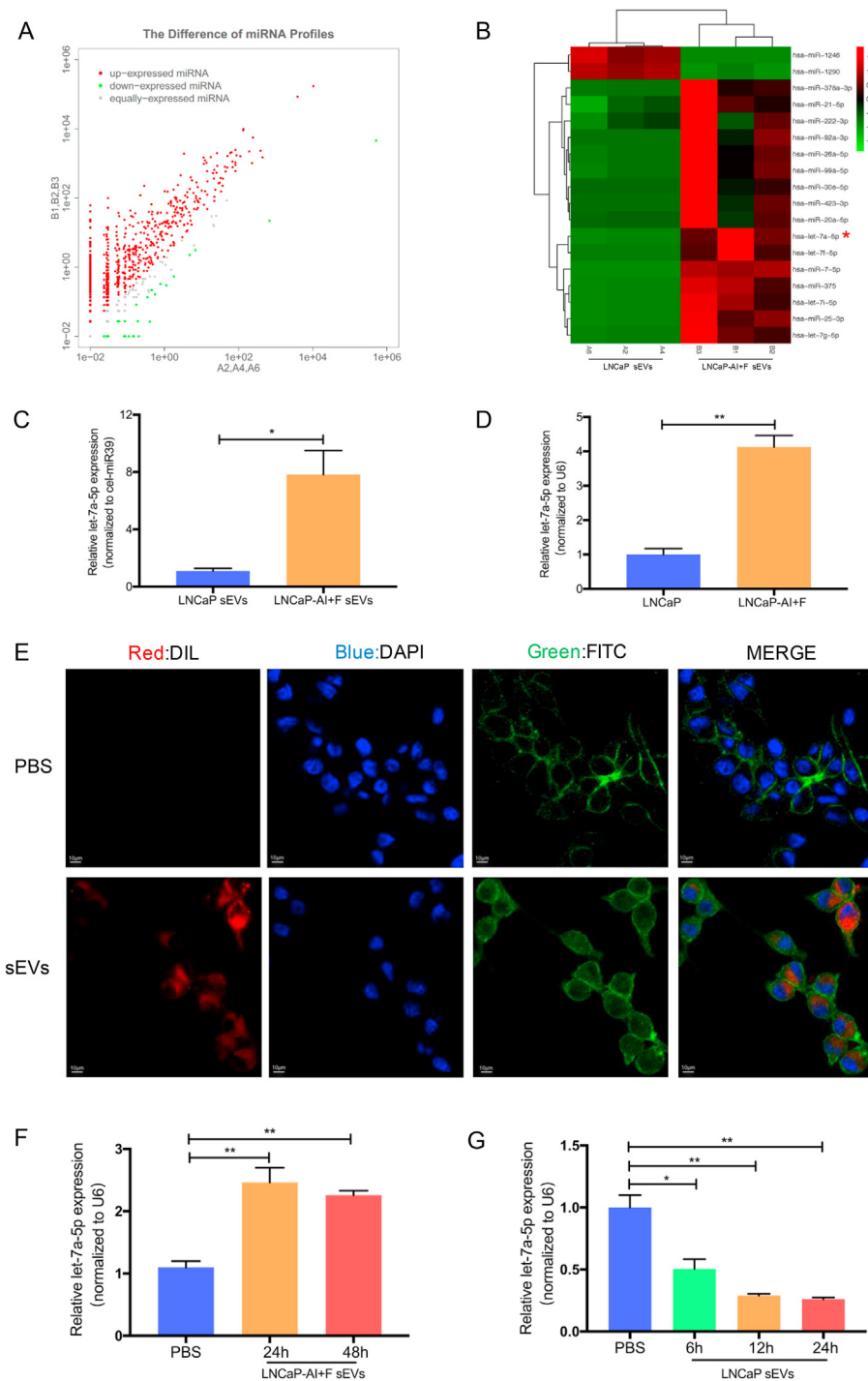


**Figure 4.** Let-7a-5p was transferred by PCa sEVs. (A) Scatter plot of differentially expressed miRNAs between LNCaP sEVs and LNCaP-AI + F sEVs. Red: increased expression; green: decreased expression; grey: equally expression. (B) Heat map of the differentially expressed sEVs miRNAs between LNCaP sEVs and LNCaP-AI + F sEVs. Red: increased expression; green: decreased expression. (C) Relative expression of let-7a-5p in LNCaP sEVs and LNCaP-AI + F sEVs detected by qRT-PCR. (D) Relative expression of let-7a-5p in LNCaP cells and LNCaP-AI + F cells detected by qRT-PCR. (E) Confocal images of LNCaP cells co-cultured with LNCaP-AI + F sEVs for 48–72 h in an androgen-deprived environment. (DIL labelled sEVs; FITC labelled LNCaP cell membranes; DAPI labelled LNCaP cell nuclei) (F) qRT-PCR analysis of the expression of let-7a-5p in LNCaP cells co-cultured with LNCaP-AI + F sEVs for 24, 48 h in an androgen-deprived environment. (G) qRT-PCR analysis of the expression of let-7a-5p in LNCaP-AI + F cells co-cultured with LNCaP sEVs for 6, 12, 24 h in an androgen-deprived environment. sEVs: small extracellular vesicles. Data were analyzed using *t*-test (C, D) and one-way ANOVA with multiple-comparisons test (F, G). \*,  $P < 0.05$ ; \*\*,  $P < 0.01$ ; \*\*\*,  $P < 0.001$ .

new mechanism of the AIPC transformation and a new promising therapeutic/diagnostic target for CRPC.

AR, the primary regulator for PSA expression, induces PSA expression and promotes cell proliferation through interactions with three androgen response elements [19]. However, in this study, there were a higher AR and a lower PSA protein expression in advanced LNCaP-AI + F cells than in primary LNCaP cells (Figure 1A). Meanwhile, in LNCaP-AI + F sEVs we found the similar phenomenon (Figure S1A). This apparent inconsistency can be explained; during PCa progression, PSA expression was lower in malignant cells than in the normal prostatic epithelial cells [20]. PSA was further reduced in poorly differentiated/more aggressive tumours, despite the high serum PSA levels in patients with PCa [21]. Thus, it is

notable that multiple factors are involved in the transcriptional activation of PSA, not only AR but also several growth factors and extracellular matrix proteins [22]. Our results not only proved that AIPC cells had a high AR expression but also a high *p*-Akt/Akt ratio, which is consistent with previous results [23].

There have been several studies about sEVs cargoes as potential CRPC biomarkers [24, 25, 26]. We found that crucial AR protein had higher expression on LNCaP-AI + F sEVs, which may act as the cargo transferring key messages. However, until now, how PCa sEVs regulate the castration resistance has received little attention. Zhang et al. reported that PC3 (AIPC) sEVs boosted the AIPC transition by activating HMOX1 [27]. However, the biggest issue is that the two PCa cell lines (PC3 as AIPC cells

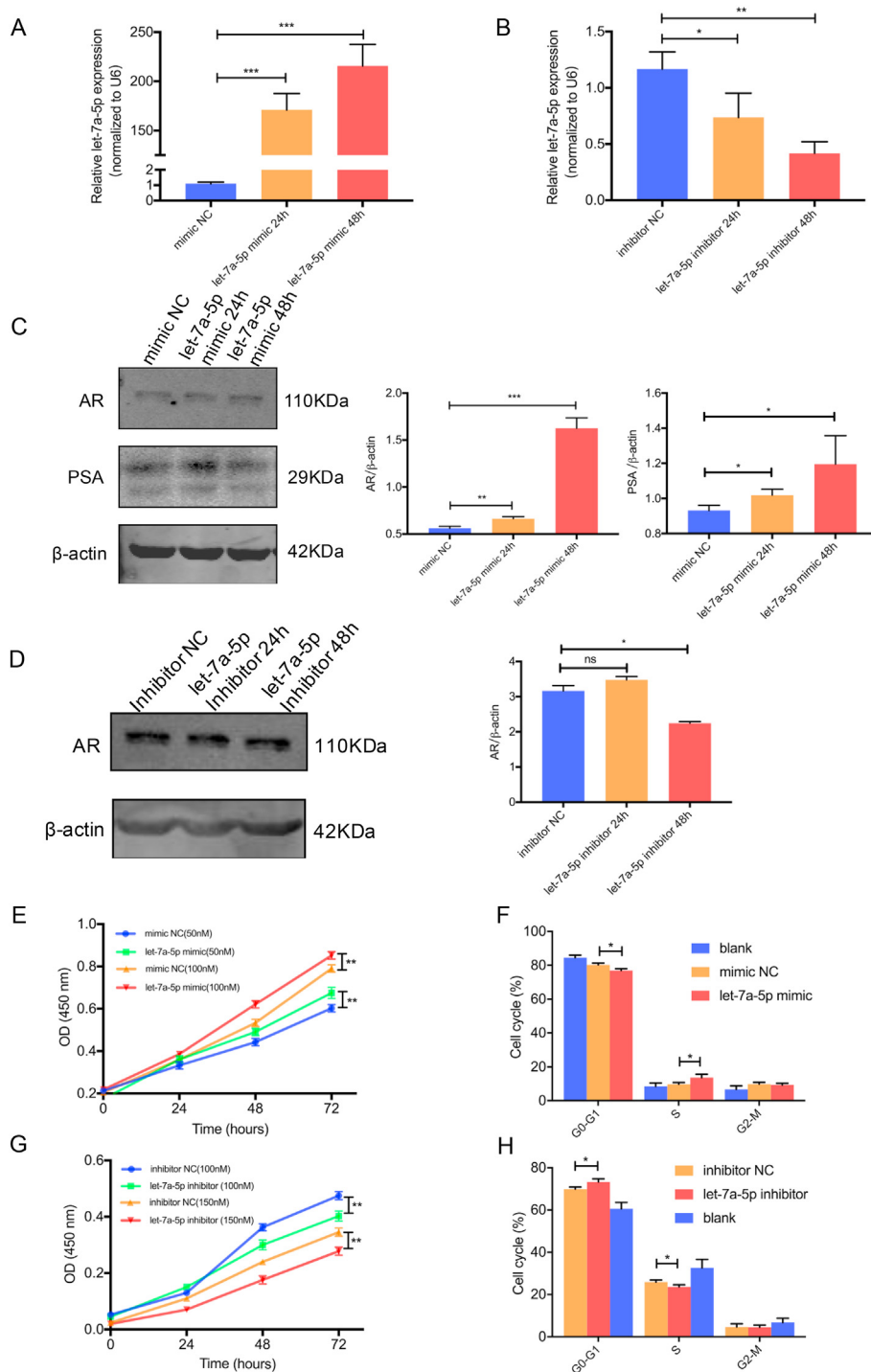


**Figure 5.** Let-7a-5p regulates the development of castration resistance in PCa cells via AR signaling. (A) qRT-PCR analysis of relative let-7a-5p expression in LNCaP cells transfected with 50 nM let-7a-5p mimic for 24 and 48 h (B) qRT-PCR analysis of relative let-7a-5p expression in LNCaP-AI + F cells transfected with 100 nM let-7a-5p inhibitor for 24 and 48 h. (C) Western blotting analysis of the protein expression of AR and PSA in LNCaP cells transfected with 50 nM let-7a-5p mimic for 24 and 48 h. Original gel data in Supplementary Materials (Figure S7). (D) Western blotting analysis of AR expression in LNCaP-AI + F cells transfected with 100 nM let-7a-5p inhibitor for 24 and 48 h. Original gel data in Supplementary Materials (Figure S8). (E) CCK-8 assay of the proliferation of LNCaP cells transfected with 50 nM, 100 nM let-7a-5p mimic for 0, 24, 48, 72 h in an androgen-deprived environment. (F) Cell cycle distributions of LNCaP cells transfected with 50 nM let-7a-5p mimic for 48 h were analysed by flow cytometry in androgen-deprived environment. (G) CCK-8 assay of the proliferation of LNCaP-AI + F cells transfected with 100 nM, 150 nM let-7a-5p inhibitor for 0, 24, 48, and 72 h in an androgen-deprived environment. (H) Cell cycle distributions of LNCaP-AI + F cells transfected with 100 nM let-7a-5p inhibitor for 48 h were analysed by flow cytometry in an androgen-deprived environment. Data were analyzed using one-way ANOVA with multiple-comparisons test. \*,  $P < 0.05$ ; \*\*,  $P < 0.01$ ; \*\*\*,  $P < 0.001$ .

and LNCaP as ADPC cells) used are different in genetic background [28], which makes the findings of this study less generalisable. On the other hand, they only demonstrated that PC3 sEVs could facilitate the AIPC transformation, but there was no evidence to substantiate the opposite.

In this study, using next generation sequencing technology to detect differential expressed sEVs miRNAs between ADPC sEVs and AIPC sEVs, we confirmed upregulation of miR-7, miR-375, and let-7a-5p in LNCaP-AI + F sEVs by qPCR. However, among the three we focused our attention, let-7a-5p was the only one showing biological function of AIPC transformation. For the first time, we showed a correlation of let-7a-5p with CRPC and we found that let-7a-5p can promote AIPC transformation by up-regulation of AR expression and p-Akt/Akt ratio.

Although, further studies need to be performed to deeply investigate the detailed target genes of let-7a-5p for AIPC transformation.

At present, most of the mechanisms responsible for progression to CRPC relates to maintenance of AR signaling and AR inhibitors as a key therapeutic target [29]. Multiple growth-promoting and survival pathways in PCa suggest the importance of alternative mechanisms involved in disease progression, such as DNA damage response pathway, PTEN/PI3K/AKT/mTOR pathway, cell cycle pathway, WNT pathway, TMPRSS2/ETS fusion, neuroendocrine pattern, and immune system response [15, 30, 31]. In this study, we demonstrated that PCa sEVs transferring let-7a-5p tune AIPC transformation by regulating AR signaling and downstream PI3K/AKT signaling.

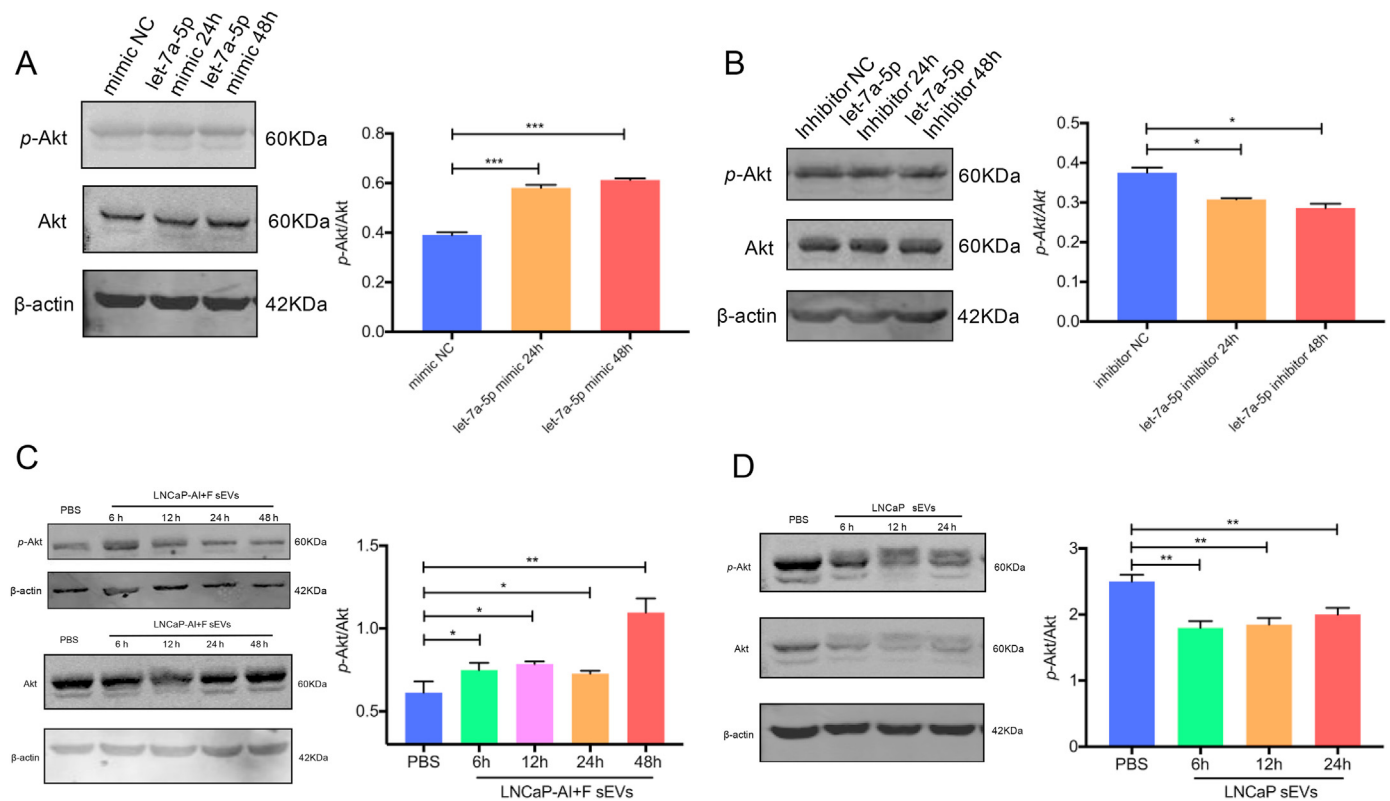


**Figure 6.** sEVs encapsulating let-7a-5p regulate the PI3K/Akt signaling pathway. (A) Western blotting analysis of the p-Akt and Akt protein expression in LNCaP cells transfected with 50 nM let-7a-5p mimic for 24 and 48 h. Original gel data in Supplementary Materials (Figure S9). (B) Western blotting analysis of the p-Akt and Akt protein expression in LNCaP-AI + F cells transfected with 100 nM let-7a-5p inhibitor for 24 and 48 h. Original gel data in Supplementary Materials (Figure S10). (C) Western blotting analysis of the p-Akt and Akt protein expression in LNCaP cells co-cultured with LNCaP-AI + F sEVs for 6, 12, 24, 48 h. Original gel data in Supplementary Materials (Figure S11). (D) Western blotting analysis of the p-Akt and Akt protein expression in LNCaP-AI + F cells co-cultured with LNCaP sEVs for 6, 12, 24 h. Original gel data in Supplementary Materials (Figure S12). sEVs: small extracellular vesicles. Data were analyzed using one-way ANOVA with multiple-comparisons test. \*,  $P < 0.05$ ; \*\*,  $P < 0.01$ ; \*\*\*,  $P < 0.001$ .

Our study not only provided new insights in CRPC development, but also provided a potential diagnostic or therapeutic target for CRPC. However, the present study still has several limitations; we will look for let-7a-5p target genes associating with AR and PI3K/Akt pathway as well as deeply investigate the underlying mechanism during CRPC development. Furthermore, it's ongoing an *in-vivo* study to confirm the *in-vitro* results.

## Declarations

### Author contribution statement

Lin Lei: Conceived and designed the experiments; Performed the experiments; Analyzed and interpreted the data.

Lijuan Yu: Conceived and designed the experiments; Contributed reagents, materials, analysis tools or data; Wrote the paper.

Weixiao Fan: Conceived and designed the experiments; Performed the experiments.

Xiaoke Hao: Conceived and designed the experiments; Contributed reagents, materials, analysis tools or data.

### Funding statement

Dr. Lijuan Yu was supported by National Natural Science Foundation of China [82203711], China Postdoctoral Science Foundation [2021M701631].

Dr. Xiaoke Hao was supported by National Natural Science Foundation of China [81872347].

### Data availability statement

Data will be made available on request.

### Declaration of interest's statement

The authors declare the following conflict of interests: L.Y. and X.H. are co-inventors on several patents about tumor exosomes. The other authors declare that there are no financial, personal, or professional interests that could be construed to have influenced the paper.

### Additional information

Supplementary content related to this article has been published online at <https://doi.org/10.1016/j.heliyon.2022.e12114>.

### Acknowledgements

We thank professor Zihua Tao at Zhejiang University for providing the LNCaP AI + F cell line gratefully. We also thank Massimo Micaroni at Gothenburg University for his critical revision on the manuscript. We are grateful for the support by International Cultivation Program for Excellent Young Talents of Guangdong Province to L.Y.

### References

- [1] R.L. Siegel, K.D. Miller, H.E. Fuchs, A. Jemal, *Cancer statistics, 2021*, *CA A Cancer J. Clin.* 71 (1) (2021 Jan) 7–33. PMID: 33433946.
- [2] M.D. Charles Huggins, V. Clarence, M.D. Hodges, *Huggins studies on prostatic cancer*, *Cancer Res.* 1 (1941) 293–297.

- [3] Y.W. Lin, Y.C. Wen, C.Y. Chu, M.C. Tung, Y.C. Yang, K.T. Hua, K.F. Pan, M. Hsiao, W.J. Lee, M.H. Chien, Stabilization of ADAM9 by N- $\alpha$ -acetyltransferase 10 protein contributes to promoting progression of androgen-independent prostate cancer, *Cell Death Dis.* 11 (7) (2020 Jul 27) 591. PMID: 32719332.
- [4] R. Ferraldeschi, J. Welti, J. Luo, G. Attard, J.S. de Bono, Targeting the androgen receptor pathway in castration-resistant prostate cancer: progresses and prospects, *Oncogene* 34 (14) (2015 Apr 2) 1745–1757. PMID:24837363.
- [5] Q. Wang, W. Li, Y. Zhang, X. Yuan, K. Xu, J. Yu, Z. Chen, R. Beroukhi, H. Wang, M. Lupien, T. Wu, M.M. Regan, C.A. Meyer, J.S. Carroll, A.K. Manrai, O.A. Jänne, S.P. Balk, R. Mehra, B. Han, A.M. Chinnaiyan, M.A. Rubin, L. True, M. Fiorentino, C. Fiore, M. Loda, P.W. Kantoff, X.S. Liu, M. Brown, Androgen receptor regulates a distinct transcription program in androgen-independent prostate cancer, *Cell* 138 (2) (2009 Jul 23) 245–256. PMID:19632176.
- [6] D. Kim, C.W. Gregory, F.S. French, G.J. Smith, J.L. Mohler, Androgen receptor expression and cellular proliferation during transition from androgen-dependent to recurrent growth after castration in the CWR22 prostate cancer xenograft, *Am. J. Pathol.* 160 (1) (2002 Jan) 219–226. PMID: 11786415.
- [7] P.P. Banerjee, S. Banerjee, T.R. Brown, B.R. Zirkin, Androgen action in prostate function and disease, *Am. J. Clin. Exp. Urol.* 6 (2) (2018 Apr 1) 62–77. PMID: 29666834.
- [8] A. Zijlstra, D. Di Vizio, Size matters in nanoscale communication, *Nat. Cell Biol.* 20 (3) (2018 Mar) 228–230. PMID: 29476154.
- [9] H. Valadi, K. Ekström, A. Bossios, M. Sjöstrand, J.J. Lee, J.O. Lötvall, Exosome-mediated transfer of mRNAs and microRNAs is a novel mechanism of genetic exchange between cells, *Nat. Cell Biol.* 9 (6) (2007 Jun) 654–659. PMID:17486113.
- [10] H. Peinado, M. Alečković, S. Lavotshkin, I. Matei, B. Costa-Silva, G. Moreno-Bueno, M. Hergueta-Redondo, C. Williams, G. García-Santos, C. Ghajar, A. Ntadori-Hoshino, C. Hoffman, K. Badal, B.A. Garcia, M.K. Callahan, J. Yuan, V.R. Martins, J. Skog, R.N. Kaplan, M.S. Brady, J.D. Wolchok, P.B. Chapman, Y. Kang, J. Bromberg, D. Lyden, Melanoma exosomes educate bone marrow progenitor cells toward a pro-metastatic phenotype through MET, *Nat. Med.* 18 (6) (2012 Jun) 883–891. PMID:22635005.
- [11] A. Hoshino, B. Costa-Silva, T.L. Shen, G. Rodrigues, A. Hashimoto, M. Tesic Mark, H. Molina, S. Kohsaka, A. Di Giannatale, S. Ceder, S. Singh, C. Williams, N. Soplop, K. Uryu, L. Pharmed, T. King, L. Bojmar, A.E. Davies, Y. Ararso, T. Zhang, H. Zhang, J. Hernandez, J.M. Weiss, V.D. Dumont-Cole, K. Kramer, L.H. Wexler, A. Narendran, G.K. Schwartz, J.H. Healey, P. Sandstrom, K.J. Labori, E.H. Kure, P.M. Grandgenett, M.A. Hollingsworth, M. de Sousa, S. Kaur, M. Jain, K. Malloy, S.K. Batra, W.R. Jarnagin, M.S. Brady, O. Fodstad, V. Muller, K. Pantel, A.J. Minn, M.J. Bissell, B.A. Garcia, Y. Kang, V.K. Rajasekhar, C.M. Ghajar, I. Matei, H. Peinado, J. Bromberg, D. Lyden, Tumour exosome integrins determine organotropic metastasis, *Nature* 527 (7578) (2015 Nov 19) 329–335. PMID:26524530.
- [12] G. Rodrigues, A. Hoshino, C.M. Kenific, I.R. Matei, L. Steiner, D. Freitas, H.S. Kim, P.R. Oxley, I. Scandariato, I. Casanova-Salas, J. Dai, C.R. Badwe, B. Gril, M. Tesic Mark, B.D. Dill, H. Molina, H. Zhang, A. Benito-Martin, L. Bojmar, Y. Ararso, K. Offer, Q. LaPlant, W. Buehring, H. Wang, X. Jiang, T.M. Lu, Y. Liu, J.K. Sabari, S.J. Shin, N. Narula, P.S. Ginter, V.K. Rajasekhar, J.H. Healey, E. Meylan, B. Costa-Silva, S.E. Wang, S. Rafii, N.K. Altorki, C.M. Rudin, D.R. Jones, P.S. Steeg, H. Peinado, C.M. Ghajar, J. Bromberg, M. de Sousa, D. Pisapia, D. Lyden, Tumour exosomal CEMIP protein promotes cancer cell colonization in brain metastasis, *Nat. Cell Biol.* 21 (11) (2019 Nov) 1403–1412. PMID:31685984.
- [13] L. Yu, B. Sui, W. Fan, L. Lei, L. Zhou, L. Yang, Y. Diao, Y. Zhang, Z. Li, J. Liu, X. Hao, Exosomes derived from osteogenic tumor activate osteoclast differentiation and concurrently inhibit osteogenesis by transferring COL1A1-targeting miRNA-92a-1-5p, *J. Extracell. Vesicles* 10 (3) (2021 Jan), e12056. PMID:33489015.
- [14] G. Xu, J. Wu, L. Zhou, B. Chen, Z. Sun, F. Zhao, Z. Tao, Characterization of the small RNA transcriptomes of androgen dependent and independent prostate cancer cell line by deep sequencing, *PLoS One* 5 (11) (2010 Nov 30), e15519. PMID: 21152091.
- [15] I.S. Vlachos, K. Zagganas, M.D. Paraskevopoulou, G. Georgakilas, D. Karagkouni, T. Vergoulis, T. Dalamagas, A.G. Hatzigeorgiou, DIANA-miRPath v3.0: deciphering microRNA function with experimental support, *Nucleic Acids Res.* 43 (W1) (2015 Jul 1) W460–W466. PMID:25977294.
- [16] C. Thomas, F. Lamoureux, C. Crafter, B.R. Davies, E. Beraldi, L. Fazli, S. Kim, D. Thaper, M.E. Gleave, A. Zoubeidi, Synergistic targeting of PI3K/AKT pathway and androgen receptor axis significantly delays castration-resistant prostate cancer progression in vivo, *Mol. Cancer Therapeut.* 12 (11) (2013 Nov) 2342–2355. PMID: 23966621.
- [17] Shorning By, M.S. Dass, M.J. Smalley, H.B. Pearson, The PI3K-AKT-mTOR pathway and prostate cancer: at the crossroads of AR, MAPK, and WNT signaling, *Int. J. Mol. Sci.* 21 (12) (2020 Jun 25) 4507. PMID:32630372.
- [18] W.G. Nelson, Commentary on huggins and hodge: 'studies on prostatic cancer, *Cancer Res.* 76 (2) (2016 Jan 15) 186–187. PMID: 26773095.
- [19] K.B. Cleutjens, H.A. van der Korput, C.C. van Eekelen, H.C. van Rooij, P.W. Faber, J. Trapman, An androgen response element in a far upstream enhancer region is essential for high, androgen-regulated activity of the prostate-specific antigen promoter, *Mol. Endocrinol.* 11 (2) (1997 Feb) 148–161. PMID:9013762.
- [20] P.J. Russell, E.A. Kingsley, Human prostate cancer cell lines, in: *Prostate Cancer Methods and Protocols*, Springer, 2003, pp. 21–39.
- [21] J.M. Mattsson, P. Laakkonen, U.H. Stenman, H. Koistinen, Antiangiogenic properties of prostate-specific antigen (PSA), *Scand. J. Clin. Lab. Invest.* 69 (4) (2009) 447–451. PMID:19551556.
- [22] Y. Guo, R. Pili, A. Passaniti, Regulation of prostate-specific antigen gene expression in LNCaP human prostatic carcinoma cells by growth, dihydrotestosterone, and extracellular matrix, *Prostate* 24 (1) (1994) 1–10. PMID:7507237.
- [23] H.P. Lin, C.Y. Lin, P.H. Hsiao, H.D. Wang, S.S. Jiang, J.M. Hsu, W.T. Jim, M. Chen, H.J. Kung, C.P. Chuu, Difference in protein expression profile and chemotherapy drugs response of different progression stages of LNCaP sublines and other human prostate cancer cells, *PLoS One* 8 (12) (2013 Dec 5), e82625. PMID: 24349321.
- [24] X. Huang, T. Yuan, M. Liang, M. Du, S. Xia, R. Dittmar, D. Wang, W. See, B.A. Costello, F. Quevedo, W. Tan, D. Nandy, G.H. Bevan, S. Longenbach, Z. Sun, Y. Lu, T. Wang, S.N. Thibodeau, L. Boardman, M. Kohli, L. Wang, Exosomal miR-1290 and miR-375 as prognostic markers in castration-resistant prostate cancer, *Eur. Urol.* 67 (1) (2015 Jan) 33–41. PMID: 25129854.
- [25] M. Del Re, E. Biasco, S. Crucitta, L. Derosa, E. Rofi, C. Orlandini, M. Miccoli, L. Galli, A. Falcone, G.W. Jenster, R.H. van Schaik, R. Danesi, The detection of androgen receptor splice variant 7 in plasma-derived exosomal RNA strongly predicts resistance to hormonal therapy in metastatic prostate cancer patients, *Eur. Urol.* 71 (4) (2017 Apr) 680–687. PMID: 27733296.
- [26] T. Guo, Y. Wang, J. Jia, X. Mao, E. Stankiewicz, G. Scandura, E. Burke, L. Xu, J. Marzec, C.R. Davies, J.J. Lu, P. Rajan, A. Grey, K. Tipples, J. Hines, S. Kudahetti, T. Oliver, T. Powles, C. Alifrangis, M. Kohli, G. Shaw, W. Wang, N. Feng, J. Shamash, D. Berney, L. Wang, Y.J. Lu, The identification of plasma exosomal miR-423-3p as a potential predictive biomarker for prostate cancer castration-resistance development by plasma exosomal miRNA sequencing, *Front. Cell Dev. Biol.* 8 (2021 Jan 7), 602493. PMID: 33490068.
- [27] Y. Zhang, B. Chen, N. Xu, P. Xu, W. Lin, C. Liu, P. Huang, Exosomes promote the transition of androgen-dependent prostate cancer cells into androgen-independent manner through up-regulating the heme oxygenase-1, *Int. J. Nanomed.* 16 (2021 Jan 12) 315–327. PMID: 33469288.
- [28] P.J. Russell, E.A. Kingsley, Human prostate cancer cell lines, *Methods Mol. Med.* 81 (2003) 21–39. PMID: 12725112.
- [29] L.J. Scott, Enzalutamide: a review in castration-resistant prostate cancer, *Drugs* 78 (18) (2018 Dec) 1913–1924. PMID: 30535926.
- [30] S.C. Lim, P.J. Jansson, S.J. Assinder, S. Maleki, D.R. Richardson, Z. Kovacevic, Unique targeting of androgen-dependent and -independent AR signaling in prostate cancer to overcome androgen resistance, *Faseb. J.* 34 (9) (2020 Sep) 11511–11528. PMID:32713076.
- [31] R.S. Liao, S. Ma, L. Miao, R. Li, Y. Yin, G.V. Raj, Androgen receptor-mediated nongenomic regulation of prostate cancer cell proliferation, *Transl. Androl. Urol.* 2 (3) (2013 Sep) 187–196. PMID: 26816736.